Size- and Shape-Controlled Magnetic (Cr, Mn, Fe, Co, Ni) Oxide Nanocrystals via a Simple and General Approach

Nikhil R. Jana, Yongfen Chen, and Xiaogang Peng*

Department of Chemistry & Biochemistry, University of Arkansas, Fayetteville, Arkansas 72701

Received May 17, 2004

A general, reproducible, and simple strategy using generic chemicals is introduced for controlling the size, shape, and size distribution of oxide nanocrystals. The reaction system was generally composed of the metal fatty acid salts, the corresponding fatty acids, and a hydrocarbon solvent. The method is based on the pyrolysis of metal fatty acid salts, the most common metal compounds compatible with nonaqueous solutions. Synthesis of nearly monodisperse Fe_3O_4 nanocrystals in a large size range (3−50 nm) was developed as the model system. The method was further applied for the growth of oxide nanocrystals of the other magnetic metals in the fourth row—Cr_2O_3, MnO, Co_3O_4, and NiO nanocrystals. The size and shape control of the nanocrystals were achieved by varying the reactivity and concentration of the precursors. The reactivity was tuned by changing the chain length and concentration of the ligands, the fatty acids. Alcohols or primary amines could be used as the activation reagents when a given metal fatty acid salt was not sufficiently active under selected reaction conditions.

Introduction

Magnetic oxide nanocrystals of the elements in the fourth row of the periodic table (Cr, Mn, Fe, Co, and Ni) are important for the understanding of magnetic properties in a nanometer regime[1,2] and several technical applications,[1,3−7] ranging from magnetic resonance imaging, drug delivery, battery materials, catalysts, biosensing, to nanoelectronic materials, etc. Realization of these goals relies on the availability of size- and shape-controlled nanocrystals. To our knowledge, there is no general method reported for the synthesis of monodisperse magnetic oxide nanocrystals with size and shape control.

Colloidal magnetic oxide nanocrystals are traditionally synthesized through the precipitation of nanocrystals from basic aqueous solutions with a broad size distribtution.[8] Synthesis of oxide nanocrystals has recently been directed to nonaqueous approaches[9−19] mostly inspired by the success of the synthesis of high-quality semiconductor nanocrsystals in nonaqueous media.[20−22] The quality of the nanocrystals yielded by these nonaqueous solution methods is generally better than that of the nanocrystals synthesized in aqueous solutions. Hyeon et al.[12] reported that γ-Fe_2O_3 nanocrystals were synthesized using an organometallic compound, $Fe(CO)_5$, as the precursor and trimethylamine oxide as an oxidant in a nonaqueous solution. Recently, Sun et al. demonstrated the formation of nearly monodisperse Fe_3O_4,[13] $CoFe_2O_4$, and $MnFe_2O_4$[23] nanocrystals using metal acetylacetonates as the precursor in the presence of 1,2-hexadecanediol, oleylamine, and oleic acid in phenol ether. Yin et al.[17] reported that relatively monodisperse MnO nanocrystals were formed using manganese acetate as the precursor in a coordinating solvent composed of oleic acid and trioctylamine. The sizes of the resulting

* To whom correspondence should be addressed. Phone: 501-575-4612. E-mail: xpeng@comp.uark.edu.

(1) Kittel, C. *Introduction to Solid State Physics. Vol. 1. 6th Ed.*; Wiley: New York, 1986.
(2) Lee, G. H.; Huh, S. H.; Jeong, J. W.; Choi, B. J.; Kim, S. H.; Ri, H.-C. *J. Am. Chem. Soc.* **2002**, *124*, 12094−12095.
(3) Cotton, F. A.; Wilkinson, G.; Bochmann, M.; Murillo, C. *Advanced Inorganic Chemist, 6th Ed.*; Wiley: New York, 1999.
(4) Weissleder, R. *Radiology* **1999**, *212*, 609−614.
(5) Giraldo, O.; Brock, S. L.; Willis, W. S.; Marquez, M.; Suib, S. L.; Ching, S. *J. Am. Chem. Soc.* **2000**, *122*, 9330−9331.
(6) Tarascon, J. M.; Armand, M. *Nature* **2001**, *414*, 359−367.
(7) Patolsky, F.; Weizmann, Y.; Katz, E.; Willner, I. *Angew. Chem.* **2003**, *42*, 2372−2376.
(8) For example, Vestal, C. R.; Zhang, Z. J. *J. Am. Chem. Soc.* **2002**, *124*, 14312−14313 and references therein.
(9) Trentler, T. J.; Denler, T. E.; Bertone, J. F.; Agrawal, A.; Colvin, V. L. *J. Am. Chem. Soc.* **1999**, *121*, 1613−1614.
(10) Rockenberger, J.; Scher, E. C.; Alivisatos, A. P. *J. Am. Chem. Soc.* **1999**, *121*, 11595−11596.
(11) O'Brien, S.; Brus, L.; Murray, C. B. *J. Am. Chem. Soc.* **2001**, *123*, 12085−12086.
(12) Hyeon, T.; Lee, S. S.; Park, J.; Chang, Y.; Na, H. B. *J. Am. Chem. Soc.* **2001**, *123*, 12798−12801.
(13) Sun, S.; Zeng, H. *J. Am. Chem. Soc.* **2002**, *124*, 8204−8205.
(14) Pacholski, C.; Kornowski, A.; Weller, H. *Angew. Chem.* **2002**, *41*, 1188−1191.
(15) Urban, J. J.; Yun, W. S.; Gu, Q.; Park, H. *J. Am. Chem. Soc.* **2002**, *124*, 1186−1187.
(16) Seo, W. S.; Jo, H. H.; Lee, K.; Park, J. T. *Adv. Mater.* **2003**, *15*, 795−797.
(17) Yin, M.; O'Brien, S. *J. Am. Chem. Soc.* **2003**, *125*, 10180−10181.
(18) Lee, K.; Seo, W. S.; Park, J. T. *J. Am. Chem. Soc.* **2003**, *125*, 3408−3409.
(19) Monge, M.; Kahn, M. L.; Maisonnat, A.; Chaudret, B. *Angew. Chem.* **2003**, *42*, 5321−5324.
(20) Murray, C. B.; Norris, D. J.; Bawendi, M. G. *J. Am. Chem. Soc.* **1993**, *115*, 8706−8715.
(21) Peng, X.; Wickham, J.; Alivisatos, A. P. *J. Am. Chem. Soc.* **1998**, *120*, 5343−5344.
(22) Peng, Z. A.; Peng, X. *J. Am. Chem. Soc.* **2001**, *123*, 183−184.
(23) Sun, S.; Zeng, H.; Robinson, D. B.; Raoux, S.; Rice, P. M.; Wang, S. X.; Li, G. *J. Am. Chem. Soc.* **2004**, *126*, 273−279.

10.1021/cm049221k CCC: $27.50 © 2004 American Chemical Society
Published on Web 09/11/2004

nanocrystals in these three high-temperature and nonaqueous solution approaches were varied between a few nanometers and about 20 nm, mostly by secondary injections of the precusors—seeded growth—and Ostwald ripening. The size distribution of the magnetic oxides reported in these three papers was generally impressive, although shape control of the nanocrystals was seldomly discussed.[12,13,17] Very recently, Cheon et al. reported that, without using trimethylamine oxide as the oxidant, the organometallic approach yielded γ-Fe_2O_3 nanocrystals composed of a mixture of several different shapes.[24]

The diverse structures and properties of metal oxides make it difficult to develop a general synthetic strategy for these nanocrystals. Using an injection-hydrolysis method, O'Brien et al.[11] reported the formation of nearly monodisperse $BaTiO_3$, $PbTiO_3$, and TiO_2 nanocrystals by reacting hydrogen peroxide (30% aqueous solution) and metal−alkoxides with fatty acids as the ligands in phenol ether. The authors suggested that this approach may be developed as a general strategy for the synthesis of oxide nanocrystals. However, the instability of the precursors of this approach is a potential issue needing to be addressed.

We noticed that metal carboxylate salts, including their fatty acid salts, are the most common compounds for most metals and these compounds are compatible with nonaqueous media. In fact, our group has developed those greener synthetic approaches[25] for II−VI and III−V semiconductor nanocrystals almost exclusively based on metal carboxylate salts. It is known that metal carboxylates decompose at elevated temperatures and metal oxides are common decomposition products in many cases. All these facts encouraged us to consider a general synthetic strategy based on pyrolysis of metal fatty acid salts. The formation of MnO nanocrystals using manganese acetate as a precursor mentioned above[17] further indicates that such a route may work. Experiences have taught us that a simple system is typically easier to be understood and optimized. Considering the technical future of the oxide nanocrystals, inexpensive, safe, and air-stable chemicals have been considered as choices of the starting materials.

Colloidal II−VI semiconductor nanocrystals are the most developed ones in terms of synthetic chemistry due to the success of the organometallic approaches[20,26] and the alternative (or greener) approaches.[22,27,28] The key to this success, as revealed by the mechanism studies, is to maintain a balance between the nucleation and growth stages.[21,28,29] This balance can be better achieved by the noncoordinating solvent approaches introduced recently.[28] This is so because the reactivity of precursors in noncoordinating solvents can be fine-tuned by varying the bonding strength of the ligands to the monomers, concentration, chain length, and/or configuration of the ligands for the monomers.[28−30] The results shown below will demonstrate that this concept is also valid for the growth of oxide nanocrystals.

Experimental Section

Chemicals. Iron(III) chloride hexahydrate (97%), iron(II) chloride tetrahydrate (99%), nickel chloride hexahydrate, chromium(III) chloride (98%), decanoic acid (99%), lauric acid (99.5%), myristic acid, palmitic acid (99%), oleic acid (tech. 90%), stearic acid (95%), tetramethylammonium hydroxide pentahydrate (97%), octadecylamine (97%), manganese(II) chloride (98%), 1-octadecene (tech. 90%), and 1-octadecanol (99%) were purchased from Aldrich. Iron(II) stearate (Fe 9%), cobalt stearate, nickel stearate, zinc stearate (ZnO 12.5−14%), *n*-eicosane, and *n*-tetracosane were purchased from Alfa Aesar. All chemicals were used directly without any further purification.

General Reaction Conditions. The precursors used in this work were metal fatty acid salts, although metal oxides also worked in certain cases. Typically, reactions using metal fatty acid salts were reproducible, significantly better than the ones using metal oxide powder—dissolved by fatty acids directly in the reaction flask—as the starting material. To tune the activity of the metal fatty acid salts, a certain amount of the corresponding free fatty acids was employed as the ligands for both monomers and nanocrystals. The noncoordinating solvents were either octadecene (ODE), *n*-eicosane, tetracosane, or a mixture of ODE and tetracosane. Fatty acids with 10−18 carbon atoms per molecule were studied. Activation reagents, either primary amines or alcohols, were used in cases for accelerating the reaction rate and lowering the reaction temperature. No size sorting was applied for the samples used for the characterizations shown in this report.

Except the places stated differently, the initial concentration of the precursor—metal fatty acid salts—was fixed at 0.2 mol/kg and a certain concentration of the corresponding free acids (ranging from 0 to 2 mol/kg) were added into a chosen noncoordinating solvent (5 g). Ar flow was in place because the reaction temepratures may be above the flammable point of the organic compounds. The mixture turned to be a clear solution at around 100−200 °C. The growth temperature for the oxide nanocrystals was tested between 300 and 380 °C.

Typical Reaction for Growth of Oxide Nanocrystals without Activation Reagent (Fe_3O_4 Nanocrystals as the Example). *Step 1: Preparation of Fe(II)/Fe(III) Oleate.* Iron(II) stearate is commercially available and was used directly in the synthesis. For other iron fatty acid salts, the following procedure was used for their preparation.

5.4 g of $FeCl_3 \cdot 6H_2O$ or 4 g of $FeCl_2 \cdot 4H_2O$ was dissolved in 100 mL of methanol, and then oleic acid was added in 3 equiv (17 mL) for ferric salt and 2 equiv (11 mL) for ferrous salt. Into one of these two solutions, a NaOH solution with 2.4 g (for ferric) or 1.6 g (for ferrous) of NaOH in 200 mL of methanol was dropped under magnetic stirring conditions. The observed brown precipitate was washed with methanol 4−5 times and dried under vacuum overnight to remove all solvents.

The salts made by the above procedure (approximately 1 mmol dissolved in 10 mL of $CHCl_3$) was added dropwise into a stirred concentrate hydrochloric acid aqueous solution for digestion. The brown-colored complex was converted into faint yellow-colored iron chloride complex—which was in the aqueous phase. The colorless chloroform extract, containing carboxylic acid, was collected, dried, and weighed. Based on the results, the complex composition was determined as $Fe^{III}(oleate)_3$ or $Fe^{II}(oleate)_2$.

The brown-colored solid was dissolved in 20 mL of 1-octadecene (technical grade, 90%) at 60−70 °C and preserved as a stable stock solution at room temperature for the next step.

Step 2: Synthesis of Fe_3O_4 Nanocrystals. The Fe_3O_4 nanocrystals were prepared by the decomposition of iron−oleate complexes at 300 °C using octadecene as the solvent. The particle sizes can be controlled between 8 and 50 nm without using any activation reagent, by varying the amount of excess

(24) Cheon, J.; Kang, N.-J.; Lee, S.-M.; Lee, J.-H.; Yoon, J.-H.; Oh, S. J. *J. Am. Chem. Soc.* **2004**, *126*, 1950−1951.
(25) Peng, X. *Chem. Eur. J.* **2002**, *8*, 334−339.
(26) Peng, X.; Manna, L.; Yang, W. D.; Wickham, J.; Scher, E.; Kadavanich, A.; Alivisatos, A. P. *Nature* **2000**, *404*, 59−61.
(27) Qu, L.; Peng, Z. A.; Peng, X. *Nano Lett.* **2001**, *1*, 333−336.
(28) Yu, W. W.; Peng, X. *Angew. Chem., Int. Ed.* **2002**, *41*, 2368−2371.
(29) Yu, W. W.; Wang, Y. A.; Peng, X. *Chem. Mater.* **2003**, *15*, 4300−4308.
(30) Battaglia, D.; Peng, X. *Nano Lett.* **2002**, *2*, 1027−1030.

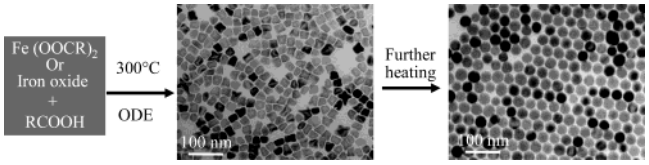

Figure 1. Schematic illustration of the formation of Fe_3O_4 nanocrystals. The middle and right panels are TEM images of the as-synthesized nanocrystals taken at different reaction times.

oleic acid, or by changing the concentration of the precursor salt during the reaction. Other nonspherical shapes such as cubes or spheroids can also be obtained by freezing the reaction at early stages.

In a typical synthesis, 1 mL of the stock solution made in the first step was mixed with 4 mL of octadecene and an appropriate amount of oleic acid (from 0.1 to 10 equiv) and the mixture was heated to 300 °C under an argon atmosphere. The reaction progress could be monitored by taking aliquots at different reaction times and observing the nanocrystals in the aliquots under TEM (JEOL 100 CX, 100 kV, copper grids coated with Formvar film). XRD was recorded using the standard methods reported previously.[31] FTIR was used to verify that the nanocrystals were coated with the corresponding fatty acid in its ionized form ($R-COO^-$).

Nanocrystals could be precipitated from the reaction mixture using a minimum amount of methanol/acetone and the precipitate was collected after centrifugation. This precipitate was re-dispersible in typical nonpolar solvents such as chloroform and toluene. The precipitation/dispersion scheme was repeated 2−3 times to purify the nanocrystals. No size sorting was applied for any samples used for the measurements to be discussed below.

The conditions for the formation of the nanocrystals with several given sizes are as follows:

8 nm size: Start with ferric oleate, use 0.1 equiv excesses oleic acid, and heat the reaction mixture for 15−30 min.

30 nm size: Start with ferric oleate, use 3 equiv excesses oleic acid, and heat the reaction for 30 min.

30 nm size cube particles: Start with ferrous oleate, use 2 equiv excesses oleic acid, and heat the reaction for 1 h.

Typical Reaction for Growth of Oxide Nanocrystals with Activation Reagents (Fe_3O_4 Nanocrystals as the Example). With use of Fe(II)−stearate as the precursor, the iron oxide nanocrystals of about 3 nm in size can be prepared by using alkylamine as the activation reagents. In a typical synthesis, 0.622 g of iron stearate and 0.269 g of octadecylamine were mixed with 5 mL of octadecene and heated to 300 °C under an argon atmosphere. The reaction was matured after 15 min of heating. Following the same procedure described above, the nanocrystals were purified and characterized.

Results and Discussions

Fe_3O_4 Nanocrystals. The Fe_3O_4 nanocrystals system was employed as a model system for studying the growth of oxide nanocrystals (Figure 1). High-temperature pyrolysis made it possible for following the temporal evolution of the size and shape of the nanocrystals because pyrolysis reaction was quenched completely by lowering the temeprature of the mixture to room temperature. Different from similar studies carried out for semiconductor nanocrystals,[20,21] the reaction was monitored by taking TEM measurements of the quenched aliquots at different reaction intervals.

To avoid the formation of oxide mixtures, the reaction temperatures were carefully controlled. For this model

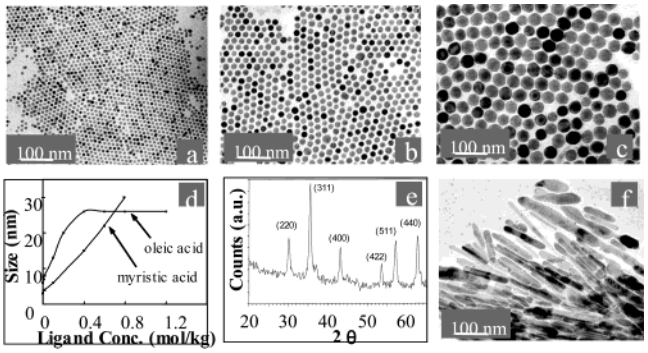

Figure 2. (a), (b), and (c) are TEM images of as-prepared dot-shaped Fe_3O_4 nanocrystals. The ligand concentration and structure dependence of the dot sizes is illustrated in (d). The X-ray powder diffraction pattern of a dot-shaped Fe_3O_4 nanocrystal is shown in (e). (f) is the TEM image of the as-prepared elongated Fe_3O_4 nanocrystals.

system, formation of nanocrystals was not observed when the temperature was below 250 °C. Below 300 °C, the reactions were still quite slow, typically taking several tens of minutes to complete. The formation of nanocrystals included several stages. In the beginning, formation of very small particles was observed after the solution was heated within about 10 min. After this initial stage, quasi-cube-shape nanocrystals with a small fraction of start-shaped ones (several of them circled in Figure 1, middle panel) were observed as the common products (Figure 1, middle). The cubes were much more stable and readily observable when a high concentration of a fatty acid with a relatively long chain was used as the ligands.

The quasi-cube nanocrystals gradually changed to nearly monodisperse dot-shaped nanocrystals (Figure 1, right) upon heating at the same temperature. The volumes of the cubes and the subsequently observed dots were approximately the same, indicating a likelihood of intraparticle ripening observed in the case of semiconductor nanocrystals.[31] The monodisperse dot nanocrystals were found to hold the size distribution for several tens of minutes. Typically, this time window increased as the chain length and/or concentration of the ligands increased. After that, the size distribution of the dot-shaped nanocrystals became more and more broad (not shown), which is likely the Ostwald ripening process.

Nearly monodisperse dot-shaped Fe_3O_4 nanocrystals were found to be achievable in the size range between about 6 and 50 nm without using any activation reagents (see examples in Figure 2, top row). Even smaller Fe_3O_4 nanocrystals were formed by adding a certain amount of activation reagents, primary amines or alcohols, into the reaction mixture prior to heating (to be discussed later). The size control of the Fe_3O_4 nanocrystals was achieved by varying the concentration and/or the chain length of the fatty acids when the monomer concentration was fixed (Figure 2d). The higher the ligand concentration, the larger the size of the nearly monodisperse nanocrystals (Figure 2). When the fatty acid with a relatively long chain was used, such as stearic acid and oleic acid, the size of the monodisperse nanocrystals achieved before the Ostwald ripening stage was almost fixed at a certain value that was dependent on the ligand concentration. However, before

(31) Peng, Z. A.; Peng, X. G. *J. Am. Chem. Soc.* **2001**, *123*, 1389−1395.

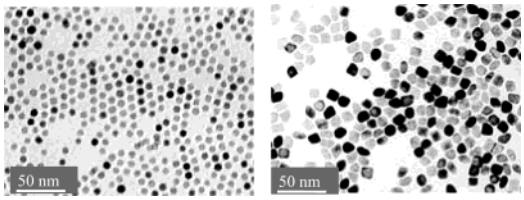

Figure 3. TEM images of as-prepared MnO nanocrystals.

defocusing of the size distribution of the nanocrystals, the size of the nearly monodisperse Fe_3O_4 nanocrystals synthesized using fatty acids with a relatively short chain length (10−14 carbon per molecule) was found to increase in a significant size range as the reaction proceeded. Generally, the overall reaction rate was accelerated by shortening the chain length, which is consistent with the decrease of the reactivity of the monomers.[29] Interestingly, if two types of fatty acids were used in a single reaction, two distinguishable sized Fe_3O_4 nanocrystals were found under TEM (data not shown).

The shape control of Fe_3O_4 nanocrystals was partially achieved. Besides the dots and the quasi-cubes (Figures 1 and 2), some Fe_3O_4 nanocrystal rods/wires were observed (Figure 2) when the ligand concentration was very high (higher than 5 times the total iron concentration in the solution) or the monomer concentration was much higher than the typical reaction. However, the yield of these elongated shapes was low and always mixed with a high population of dots.

The X-ray powder diffraction (XRD) (Figure 2) and electron diffraction patterns of Fe_3O_4 nanocrystals yielded by the thermal decomposition of either Fe(II) or Fe(III) salts were all consistent with that of Fe_3O_4 crystals. The domain size determined by the peak widths of the XRD patterns matched the size determined by the TEM measurements, indicating the single-crystalline nature of the nanocrystals. The Fe_3O_4 nanocrystals were found to be stable as a colloidal solution at room temperature. Purification of the nanocrystals was performed by the addition of acetone into the toluene/chloroform solution of the nanocrystals. Most of the precipitate would remain to be soluble in toluene/chloroform, although some nanocrystals might become insoluble, especially when the purification procedure was repeated multiple times. The precipitates appeared to be black as expected for Fe_3O_4 and responded strongly to an external magnetic field induced by a laboratory magnetic bar. The yield of Fe_3O_4 nanocrystals was high, above 85%, if the free fatty acid concentration was not too high.

Formation of MnO Nanocrystals. The formation of MnO nanocrystals was found to be very similar to that of Fe_3O_4 nanocrystals. Similar to Fe_3O_4 nanocrystals, the reaction temperature at 300 °C was sufficient. Quasi-cube and dot-shaped MnO nanocrystals were subsequently observed for this system (Figure 3). The crystal structure of the nanocrystals was found to be consistent with rock salt MnO, and the powder sample isolated from the reaction flask appeared to weakly respond to an external magnetic field induced by a laboratory magnetic bar, which is different from the antiferrimagnetic nature of the bulk MnO crystals.[2]

Co_3O_4 Nanocrystals. Co_3O_4 nanocrystals were obtained by the decomposition of Co(II) fatty acid salts.

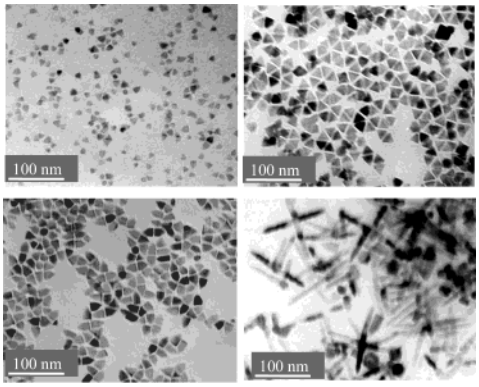

Figure 4. TEM images of the as-synthesized Co_3O_4 nanocrystals.

In comparison with that of the Fe_3O_4 and MnO nanocrystals, the formation of Co_3O_4 nanocrystals was found to be more difficult. When the reaction temperature was below 320 °C, no nanocrystal formation was observed. With use of cobalt stearate ($Co(SA)_2$) as the precursor at a concentration of 0.2 mol/kg, no particle formation was observed if the free ligand concentration was higher than approximately 0.6 mol/kg. The obtained nanocrystals were typically either triangular (top row, Figure 4), bulletlike (left bottom, Figure 4), or rod-shaped (right bottom, Figure 4). Different from the Fe_3O_4 and MnO nanocrystals, these faceted nanocrystals were very stable upon prolonged heating, for at least 5 h, and conversion to dot-shaped ones was not observed. However, these faceted shapes did become more round after some additional free fatty acids were added into a stabilized reaction system at the given reaction temperature. This implies that the stability of the faceted nanocrystals in the original reaction solution was probably due to the low fatty acid concentration allowed for the reaction system.

Nickel Oxide and Chromium Oxide Nanocrystals. Nckel Oxide and chromium oxide nanocrystals were more difficult to form in comparison with the other three types of magnetic oxide nanocrystals. The formation of NiO nanocrystals did not occur if fatty acids with a relatively long hydrocarbon chain, stearic acid or oleic acid, were used as the ligands. When nickel myristate and myristic acid were employed and a relatively high temperature (around 340 °C) was in place, the reaction yielded triangular NiO nanocrystals (Figure 5). Among all five types of magnetic oxides tested, formation of Cr_2O_3 nanocrystals was found to be most difficult. No sign of the decomposition of the precursors was observed up to 380 °C with all types of fatty acid salts tested if the system was composed of chromium fatty acid salts and noncoordinating solvents (with or without free fatty acids). As shown in Figure 5, triangular Cr_2O_3 nanocrystals were synthesized at 340 °C when a small amount of octadecylamine (0.2 mol/kg) was added into the reaction system with a precursor concentration at 0.2 mol/kg, i.e., the ratio between stearate and amine being 2:1. The precipitate of Cr_2O_3, NiO, and Co_3O_4 nanocrystals all responded to the external magnetic field induced by a laboratory magnetic bar.

We tried to extend the above approach, pyrolysis of metal fatty acid salts, to other types of oxide nanocrystals. Formation of ZnO nanocrystals (Figure 5)—an

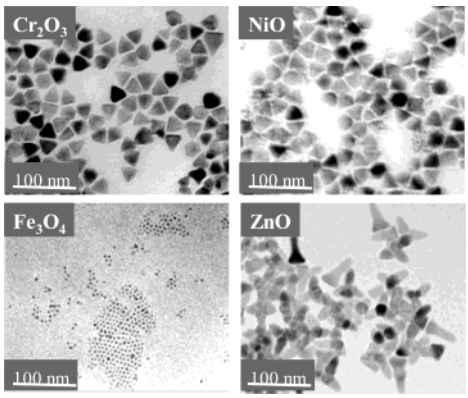

Figure 5. TEM images of different types of oxide nanocrystals. Except NiO nanocrystals, the other nanocrystals shown here were all formed by catalytic reactions.

example of technically important wide band gap semiconductor[14,19,32,33]—was observed when a small amount of amine or alcohol was added into the system. In addition to the pseudo bullet-shaped ZnO nanocrystals (Figure 5), preliminary results further revealed that nearly monodisperse triangle- and dot-shaped ZnO nanocrystals were also obtained (detail will be reported separately). In comparison with amines, alcohols typically are milder activating reagents.

Activating reagents, a small amount of amines or alcohols, significantly accelerated the formation of all types of magnetic oxide nanocrystals discussed above. Typically, the size of the nanocrystals was smaller if an activating reagent was in the reaction solution. This is consistent with the increased reactivity coefficient of the precursors.[29] For instance, the size of nearly monodisperse Fe_3O_4 nanocrystals could reach as small as 3−4 nm for amine-activated reactions (Figure 5). The molecular mechanism of the activating processes is under intensive study.

Conclusion

In summary, a relatively simple, reproducible, and general strategy for the growth of magnetic oxide nanocrystals based on pyrolysis of metal fatty acid salts in noncoordinating solvents is introduced. Our preliminary results also revealed that the surface ligands of these magnetic oxide nanocrystals can be readily replaced by dendron ligands, resulting in soluble and extremely stable dendron nanocrystals in a variety of solvents (will be reported separately). Provided that metal fatty acid salts are the most common, inexpensive, relatively safe, and room-temperature stable metal compounds soluble in nonaqueous solutions, this strategy may be extendable to other metal oxide nanocrystals as revealed by the preliminary results. An important concept introduced during the development of synthetic chemistry of semiconductor nanocrystals, balancing nucleation and growth by tuning the reactivity of the monomers, was verified to be valid for the formation of oxide nanocrystals. The similarity and difference on the growth of different types of oxide nanocrystals reported here might help to open a door for a general understanding of the formation of shape-controlled monodisperse inorganic nanocrystals. This new strategy is possible to be extended to a large scale, given that the process and the composition of the room-temperature stable starting materials are both simple.

Acknowledgment. Financial support from the National Science Foundation and the University of Arkansas are acknowledged.

Supporting Information Available: Additional figures (PDF). This material is available free of charge via the Internet at http://pubs.acs.org.

CM049221K

(32) Huang, M. H.; Mao, S.; Feick, H.; Yan, H.; Wu, Y.; Kind, H.; Weber, E.; Russo, R.; Yang, P. *Science* **2001**, *292*, 1897−1899.
(33) Tian, Z. R.; Voigt, J. A.; Liu, J.; McKenzie, B.; McDermott, M. J.; Rodriguez, M. A.; Konishi, H.; Xu, H. *Nat. Mater.* **2003**, *2*, 821−826.